Amide I vibrational modes in glycine dipeptide analog: Ab initio calculation studies

Sangyob Cha, Sihyun Ham, and Minhaeng Cho

Citation: The Journal of Chemical Physics **117**, 740 (2002); doi: 10.1063/1.1483257
View online: https://doi.org/10.1063/1.1483257
View Table of Contents: http://aip.scitation.org/toc/jcp/117/2
Published by the American Institute of Physics

Amide I vibrational modes in glycine dipeptide analog: *Ab initio* calculation studies

Sangyob Cha, Sihyun Ham, and Minhaeng Cho[a)]
Department of Chemistry and Center for Multidimensional Spectroscopy, Division of Chemistry and Molecular Engineering, Korea University, Seoul 136-701, Korea

(Received 18 January 2002; accepted 16 April 2002)

Coupling between two local amide I vibrational motions of peptides has been quantitatively estimated by assuming that the two peptides interact with each other via dipole–dipole interaction, the so-called transition dipole coupling (TDC) model. The TDC theory has been applied to describing amide I IR and Raman band envelopes and further used to interpret the two-dimensional IR pump–probe and photon echo spectra of polypeptides recently. In order to quantitatively test the validity of the TDC model or in general dipole–dipole interaction model for a dipeptide, we carry out systematic investigations, by using both the *ab initio* calculation methods and extended TDC theory, on the potential energy surface, vibrational frequencies of symmetric and antisymmetric amide I vibrational normal modes, transition dipole and transition polarizability, IR and Raman intensities of the two modes, IR-Raman noncoincidence phenomena in the full Ramachandran space for a model dipeptide, glycine dipeptide analog. It is found that the spectroscopic properties of dipeptide can be quantitatively well described by the TDC model, but the quantities related to the potential energy surface such as absolute magnitudes of vibrational frequencies and frequency splitting between the two normal modes cannot be accounted for by using the TDC model. A further investigation of dimeric system with two formamide molecules is presented and the applicability of the TDC model to through space vibrational interaction as a function of intermolecular distance between the two peptides is examined. © *2002 American Institute of Physics.*
[DOI: 10.1063/1.1483257]

I. INTRODUCTION

The amide I band has been known to be highly sensitive to the secondary structures of polypeptides and proteins so that it has served as a critical indicator of the presence of α helices and/or β sheets. Particularly, as emphasized by Krimm and co-workers, the sensitivity of the amide I band envelope to secondary structures has been assumed to mainly arise from electrostatic interactions between the peptide-group vibrations, which was recognized as the transition dipole coupling (TDC).[1–3] Due to the dipole–dipole interaction between any pair of peptides, coupling force constant, which is the off-diagonal element of the corresponding Hessian matrix in the subspace constructed by the amide I vibrational coordinates of each peptide bond, can be easily calculated by examining the distance and relative orientation between the two relevant peptide groups in a given polypeptide. This simplified TDC model has been found to be quantitatively reliable in describing frequency splitting phenomena observed in the IR spectra of α helices and β sheets.[2,3] A number of experimental and theoretical studies confirming the validity of the TDC model was already reported previously.[4–8]

In parallel with these investigations concerning the coupling force constants, i.e., off-diagonal Hessian matrix elements, the diagonal amide I vibrational force constants of polypeptides were also studied in detail and they appear to be strongly affected by the inter- and intramolecular interactions, such as hydrogen bonds to solvent water molecules as well as to other peptide groups.[9–15] Combining these effects altogether, one can, in principle, describe the shape and position of the amide I band for a variety of polypeptides and globular proteins consisting of varying proportions of α helices and β sheets.

Although there already exist a vast number of literatures, where a variety of attempts were made to improve the TDC model by adding additional potential functions, there does not exist systematic investigation on the spectroscopic properties of dipeptide by using the TDC model. In other words, the validity of the TDC theory, for a model dipeptide, has not been completely tested by carrying out *ab initio* calculations of frequency splitting [frequency difference between the symmetric (A-mode) and antisymmetric (E-mode) amide I vibrations], center frequency, center frequencies of the amide I IR and Raman spectra, relative IR and Raman intensities of the symmetric and antisymmetric modes, and IR-Raman noncoincidence phenomenon. In the present study, we will consider a model dipeptide, so-called glycine dipeptide (GD) analog (*N*-acetyl-*N′*-methyl glycyl amide), shown in Fig. 1(a). In order to apply the TDC theory, we assume that the GD is comprised of two *N*-methylacetamide (NMA) molecules [see Fig. 1(b)]. Then, we calculate all those quantities mentioned above in the full Ramachandran space and will show the successes and failures of the TDC model by comparing the *ab initio* calculation results with the TDC predicted quantities. This paper is organized as follows. *Ab ini-*

a)Electronic mail: mcho@korea.ac.kr

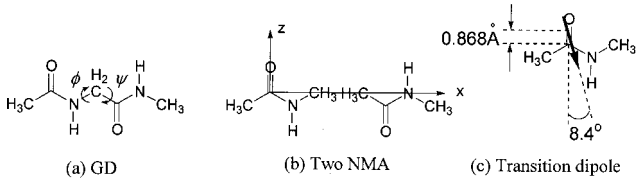

FIG. 1. Glycine dipeptide (GD) analog (*N*-acetyl-*N'*-methyl glycyl amide) (a), two NMA molecules with a chosen molecular coordinate frame (b), and the transition dipole vector of a single NMA (c).

tio calculation methods used in the present study are briefly discussed in Sec. II. An extended TDC model and a variety of quantities that can be calculated by using the TDC model are described in Sec. III. *Ab initio* calculation results and comparisons are presented in Sec. IV. Model calculation for a dimeric system consisting of two formamide molecules is presented in Sec. V. Finally, the main results are summarized in Sec. VI.

II. *AB INITIO* CALCULATION METHOD

All *ab initio* molecular orbital calculations were performed with the GAUSSIAN98 program.[16] Geometry optimization and vibrational frequency analysis were performed at the RHF/6-31++G** level. A large basis set with diffuse and polarization functions is used to provide a better description of the potential energy surface of the system. The vibrational frequencies were, as usual, corrected by multiplying the scaling factor (0.89). Partial geometry optimization of GD molecule was performed for each fixed ϕ and ψ angles (see Fig. 1). The ϕ and ψ angles were taken at intervals of 20° so that totally 324 sets of ϕ and ψ values were considered—among them 164 conformations are independent. Except ϕ and ψ dihedral angles, all other geometrical parameters were fully optimized. Also, the first-order derivatives of electric dipole and polarizability with respect to the vibrational coordinates, i.e., $(\partial\mu/\partial q_s)_0$, $(\partial\mu/\partial q_a)_0$, $(\partial\alpha/\partial q_s)_0$, and $(\partial\alpha/\partial q_a)_0$, were calculated at the RHF/6−311++G** level. Here, q_s and q_a denote the vibrational coordinates of the symmetric and antisymmetric stretching modes, respectively. For example, the symmetric mode corresponds to the vibrational motion that both carbonyl groups stretch simultaneously. As mentioned in the Introduction, the GD is assumed to be comprised of two NMA molecules so that the geometry optimization and vibrational analysis of NMA were also performed by using the same *ab initio* calculation method (see Table I). The magnitude of the transition dipole moment for NMA is calculated to be 2.70 D $\text{Å}^{-1}\,\text{amu}^{-1/2}$ and the location and direction are shown in Fig. 1(c). These results will be used to calculate various properties of dipeptide with TDC theory.

III. DIPOLE–DIPOLE-INTERACTION MODEL FOR A DIPEPTIDE

The amide I vibration of a given peptide bond is well approximated as an oscillating dipole. In this section, by assuming that the interpeptide interaction is dictated by dipole–dipole interaction, a slightly extended TDC theory will be presented.

TABLE I. Permanent dipole moment (in ea_0), polarizability (in $e^4a_0^4/E_h^2$), transition dipole (in e), and transition polarizability tensor (in $e^4a_0^2/E_h^2$) of NMA.

	μ	$(\partial\mu/\partial q)$
x	0.344	0.279
y	0.000	0.000
z	−1.588	−1.879
	α	$(\partial\alpha/\partial q)$
xx	49.643	0.743
yx	0.000	0.000
yy	37.783	−0.678
zx	−1.048	−4.195
zy	0.000	0.000
zz	45.829	6.346

A. Model Hamiltonian and normal mode analysis

The model Hamiltonian of the interacting dipoles is written as

$$H=\tfrac{1}{2}(P_1^2+\omega_1^2Q_1^2)+\tfrac{1}{2}(P_2^2+\omega_2^2Q_2^2)+V_{DD}(Q_1,Q_2), \quad (1)$$

where

$$V_{DD}(Q_1,Q_2)=\mu_1(Q_1)\cdot\tilde{T}_{12}(\phi,\psi)\cdot\mu_2(Q_2),$$
$$\tilde{T}_{12}(\phi,\psi)=\frac{1}{4\pi\varepsilon_0|\mathbf{r}|^3}[\tilde{I}-3\hat{r}\hat{r}]. \quad (2)$$

The dipole moments of the two peptides are denoted as μ_1 and μ_2, respectively. The mass-weighted amide I vibrational coordinates of the two peptides are denoted as Q_1 and Q_2. $\tilde{T}_{12}$ is the dipole–dipole interaction tensor, and $\mathbf{r}=\mathbf{r}_1-\mathbf{r}_2$, where $\mathbf{r}_i$ $(i=1,2)$ denotes the position vectors of the two dipoles, and $\hat{r}$ denotes the unit vector along the direction of $\mathbf{r}$. Now, the dipole–dipole interaction potential is Taylor expanded with respect to the two local coordinates, Q_1 and Q_2, up to the second-order terms, i.e.,

$$V_{DD}(Q_1,Q_2)\cong C_{11}Q_1^2+C_{22}Q_2^2+C_{12}Q_1Q_2+C_1Q_1+C_2Q_2+C_0, \quad (3)$$

where

$$C_{11}=\mu_1^{(2)}\cdot\tilde{T}_{12}\cdot\mu_2^{(0)}/2, \quad C_{22}=\mu_1^{(0)}\cdot\tilde{T}_{12}\cdot\mu_2^{(2)}/2,$$
$$C_{12}=\mu_1^{(1)}\cdot\tilde{T}_{12}\cdot\mu_2^{(1)}, \quad C_1=\mu_2^{(0)}\cdot\tilde{T}_{12}\cdot\mu_1^{(1)},$$
$$C_2=\mu_1^{(0)}\cdot\tilde{T}_{12}\cdot\mu_2^{(1)}, \quad \text{and} \quad C_0=\mu_1^{(0)}\cdot\tilde{T}_{12}\cdot\mu_2^{(0)}. \quad (4)$$

Here, the dipole moment of a single peptide was expanded as

$$\mu_j\cong\mu_j^{(0)}+\mu_j^{(1)}Q_j+\tfrac{1}{2}\mu_j^{(2)}Q_j^2, \quad (5)$$

where $\mu_j^{(n)}\equiv(\partial^n\mu_j/\partial Q_j^n)_0$.

Since the model Hamiltonian is quadratic with respect to the two local coordinates, Q_1 and Q_2, normal mode analysis can be easily carried out and the resultant Hamiltonian is found to be

$$H=\tfrac{1}{2}(P_+^2+\omega_+^2Q_+^2)+\tfrac{1}{2}(P_-^2+\omega_-^2Q_-^2), \quad (6)$$

where $P_{\pm}$ denote the conjugate momenta of $Q_{\pm}$. The normal mode coordinates and corresponding frequencies are given as

$$Q_{\pm} = d_1^{\pm} Q_1 + d_2^{\pm} Q_2 + \frac{\delta_{\pm}}{2\omega_{\pm}^2}, \tag{7}$$

$$\omega_{\pm}^2 = \tfrac{1}{2}\{(\omega_1^2 + 2C_{11} + \omega_2^2 + 2C_{22}) \pm \sqrt{(\omega_1^2 + 2C_{11} - \omega_2^2 - 2C_{22})^2 + 4C_{12}^2}\}. \tag{8}$$

Here, the eigenvector elements and $\delta^{\pm}$ in Eqs. (7) and (8) are

$$d_1^{\pm} = \frac{C_{12}}{\sqrt{C_{12}^2 + (\omega_1^2 + C_{11} - \omega_{\pm}^2)^2}},$$

$$d_2^{\pm} = \frac{\omega_{\pm}^2 - \omega_1^2 - C_{11}}{\sqrt{C_{12}^2 + (\omega_1^2 + C_{11} - \omega_{\pm}^2)^2}}, \tag{9}$$

$$\delta_{\pm} = C_1 d_1^{\pm} + C_2 d_2^{\pm}.$$

It should be emphasized that the two eigenvector elements $d_1^{\pm}$ and $d_2^{\pm}$ are different from those of a conventional TDC model, where in the latter case $d_1^{\pm} = \pm 1/\sqrt{2}$ and $d_2^{\pm} = \pm 1/\sqrt{2}$. This is because the extended TDC model Hamiltonian, Eq. (1), contains additional terms, C_{11} and C_{22}, in the diagonal part of the Hessian matrix, which are originated from the dipole–dipole interaction potential. Note that these factors were previously ignored.

B. Frequency splitting and center frequency

Because of the dipolar coupling between the two amide I local modes, the amide I band of a dipeptide consists of two peaks and the magnitude of the frequency splitting has been extensively investigated by employing the TDC theory. From Eq. (7), the frequency splitting, denoted as $\delta\omega$, is given as

$$\delta\omega(\phi,\psi) \equiv \omega_+ - \omega_- \cong \frac{\sqrt{(\omega_1^2 + 2C_{11} - \omega_2^2 - 2C_{22})^2 + 4C_{12}^2}}{2\sqrt{(\omega_1^2 + \omega_2^2)/2}}. \tag{10}$$

Here, it should be noted that the TDC model initially proposed by Krimm and co-workers ignored the contributions to the diagonal force constants induced by the dipole–dipole interaction between two amide I vibrations.[2] Thus, for a homodipeptide, i.e., $\omega_1^2 = \omega_2^2$, the frequency splitting was approximated to be $\delta\omega \cong C_{12}/\omega_1$ within the conventional TDC model.

Before we proceed to the next subject, it should be clarified that two different notations referring to the two normal modes are used in the present paper. As mentioned in Sec. II, vibrational analysis of a dipeptide provides information on the two normal modes, symmetric and antisymmetric modes denoted as q_s and q_a, respectively. On the other hand, in this section, two normal coordinates were denoted as Q_+ and Q_-. These two coordinates are not identical to q_s and q_a, because the eigenvector elements, for Q_+ as an example, d_1^+ and d_2^+, can have different signs depending on the three-dimensional (3-D) conformation of dipeptide. Thus, using the following identities: $q_s = Q_+$ and $q_a = Q_-$ if $\mathrm{sgn}(d_1^+) = \mathrm{sgn}(d_2^+)$ and $q_s = Q_-$ and $q_a = Q_+$ if $\mathrm{sgn}(d_1^-) = \mathrm{sgn}(d_2^-)$, we will consistently use q_s and q_a notation, when the two normal modes are referred to hereafter.

Often, the frequency splitting is small in comparison to the vibrational (both homogeneous and inhomogeneous) dephasing constant so that the amide I band of a dipeptide appears as a single band. Thus, the center frequency, denoted as ω_{center}, can be a critical quantity revealing the nature of secondary structures in polypeptides, e.g., an α helix or β sheet. From Eq. (7), the center frequency, which is just an arithmetic mean value of ω_+ and ω_-, is found to be

$$\omega_{\mathrm{center}}(\phi,\psi) \equiv (\omega_+ + \omega_-)/2 \cong \sqrt{(\omega_1^2 + \omega_2^2 + C_{11} + C_{22})/2}. \tag{11}$$

Note that the right-hand side of Eq. (11) is fully determined by the properties of a single peptide, which is NMA in our case. If the comparison between the *ab initio* calculated ω_{center} and Eq. (11) is quantitatively acceptable, the idea that the amide I band of a polypeptide can be described by using the vibrational and electronic properties of a single prototype peptide such as NMA can be applied to the calculations of a variety of spectroscopic properties of polypeptides. This will be critically examined in Sec. IV.

C. Transition dipole moment of a model dipeptide: IR intensity

The amide I IR band of a dipeptide consists of two contributions from the IR transitions of Q_+ and Q_- modes. By using the normal mode analysis results in Sec. III A, the transition dipole moments of the two modes can be approximated as

$$\left(\frac{\partial\mu}{\partial Q_+}\right)_0 \cong d_1^+(\phi,\psi)\left(\frac{\partial\mu_1}{\partial Q_1}\right)_0 + d_2^+(\phi,\psi)\left(\frac{\partial\mu_2}{\partial Q_2}\right)_0, \tag{12a}$$

$$\left(\frac{\partial\mu}{\partial Q_-}\right)_0 \cong d_1^-(\phi,\psi)\left(\frac{\partial\mu_1}{\partial Q_1}\right)_0 + d_2^-(\phi,\psi)\left(\frac{\partial\mu_2}{\partial Q_2}\right)_0. \tag{12b}$$

Again, it should be noted that the right-hand sides of Eqs. (12) are determined by the transition dipole moment of a single peptide and the relative orientation and distance between the two peptides.

D. Transition polarizability of a model dipeptide: Raman intensity

In order to calculate the Raman intensities of the Q_+ and Q_- modes, the transition polarizabilities of a dipeptide should be calculated as

$$\left(\frac{\partial\alpha}{\partial Q_+}\right)_0 \cong d_1^+(\phi,\psi)\left(\frac{\partial\alpha_1}{\partial Q_1}\right)_0 + d_2^+(\phi,\psi)\left(\frac{\partial\alpha_2}{\partial Q_2}\right)_0, \tag{13a}$$

$$\left(\frac{\partial\alpha}{\partial Q_-}\right)_0 \cong d_1^-(\phi,\psi)\left(\frac{\partial\alpha_1}{\partial Q_1}\right)_0 + d_2^-(\phi,\psi)\left(\frac{\partial\alpha_2}{\partial Q_2}\right)_0. \tag{13b}$$

Because of the differences between the transition dipole moments in Eqs. (12) and the transition polarizability in Eqs. (13), the shape and center frequency of the amide I IR band of a dipeptide are different from those of the amide I Raman

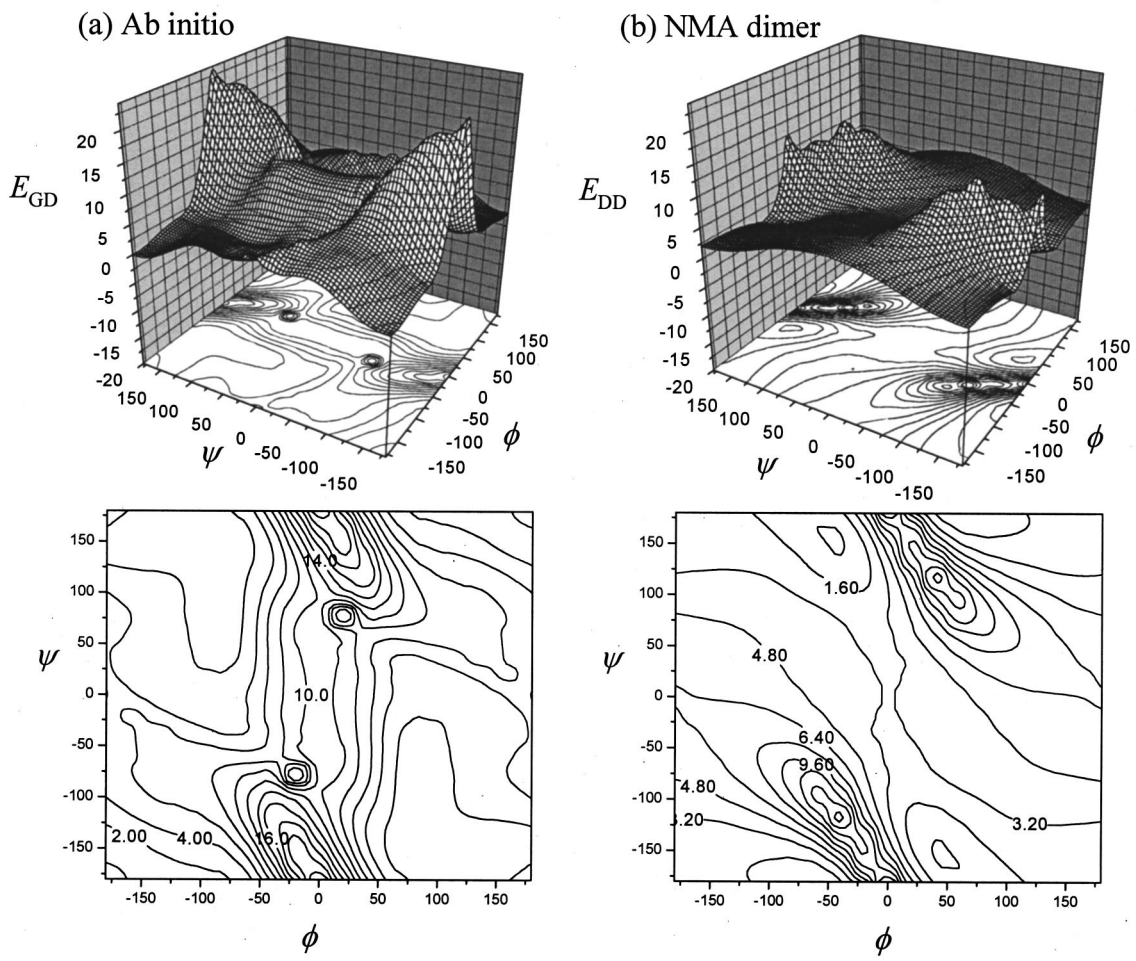

FIG. 2. (a) Potential energy surface (in kcal/mol) of GD in the (ϕ, ψ) space calculated by using the *ab initio* calculation method. (b) The dipole–dipole interaction potential energy surface for a NMA-dimer-approximated GD.

band. This noncoincidence phenomenon will be quantitatively discussed in Sec. IV D, by comparing IR and Raman center frequencies.

IV. *AB INITIO* CALCULATION RESULTS AND A COMPARISON WITH TDC MODEL PREDICTION

In this section, the *ab initio* calculation results will be directly compared with the TDC-model-predicted values.

A. Potential energy surface, permanent dipole moment, and polarizability of GD

First of all, the potential energy surface of GD, calculated at the RHF/6-311++G** level, is shown in Fig. 2(a). In fact, the same molecule was theoretically studied previously by Schafer and co-workers with the lower level of basis set, 4-21 G.[17,18] They refined four conformations with the most stable conformation (C_7) containing a seven-membered ring closed by an intramolecular hydrogen bond. Krimm *et al.* used two energy-minima conformations (C_7 and C_5) to generate vibrational force field for a dipeptide model.[19] Our higher level of calculation, with two dihedral angle constrains, found that C_5 (−180, 180) conformer is the global minimum structure and the C_7 (−80, 80) conformer is a local minimum with 0.54 kcal/mol higher in energy, as indicated in Fig. 2(a). Although there is 23.3 kcal/mol energy difference between the lowest- and highest-energy structure in the (ϕ, ψ) map, the energy differences in the available secondary structure regions of proteins are within 10 kcal/mol with a β-sheet region slightly lower in energy than the α-helical region. Since the conformational analysis of GD was already studied before, we shall not further discuss the structural aspect of GD, but the readers refer to Refs. 17, 18 for a more detailed description along this line.

We next calculate the potential energy surface, assuming that the potential function is given by Eq. (2), where the *ab initio* calculated permanent dipole moment of NMA is used (see Table I). As can be seen in Figs. 2(a) and 2(b), the overall landscapes of the *ab initio* calculated and dipole–dipole-interaction potential surfaces are similar to each other. However, the quantitative comparison (compare the two contour plots) already shows some deviations, which are originated from complicating intromolecular hydrogen bonding and steric interactions.

Now, we calculate the permanent dipole moment of GD and its norm is plotted in Fig. 3(a) in the Ramachandran space. On the basis of the assumption stated in Sec. II is correct, the permanent dipole moment of GD is just a sum of the two dipole moments of NMA1 and NMA2 [see Fig.

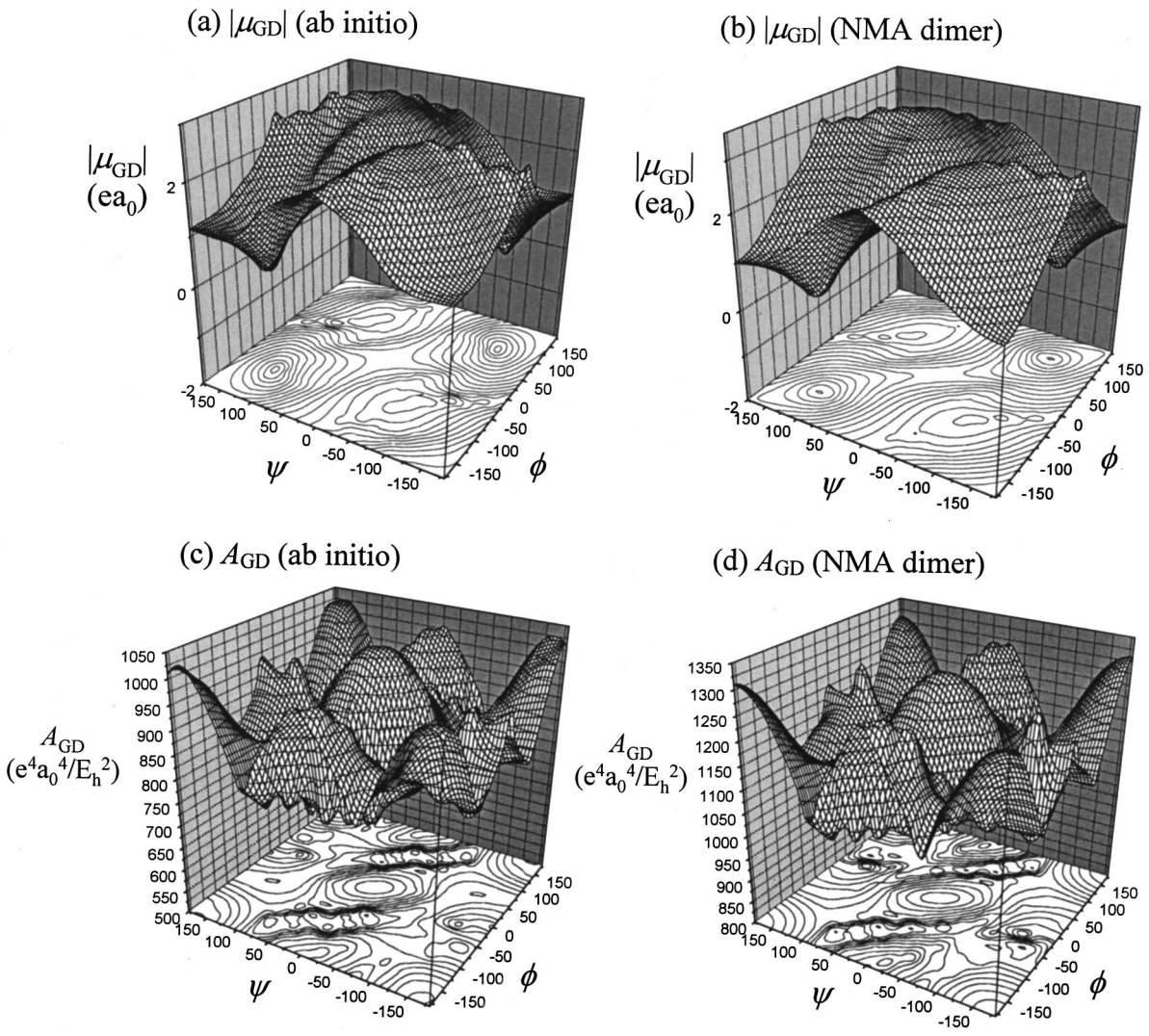

FIG. 3. Permanent dipole moment (μ in ea_0) and A (in $e^4a_0^4/E_h^2$) of GD in the (ϕ, ψ) space [see Eqs. (14) and (15) and the main context for the definition of A]. *Ab initio* calculation results of $|\mu_{GD}|$ and A_{GD} are depicted in panels (a) and (c), respectively. $|\mu_{GD}|$ and A_{GD} of NMA-dimer-approximated GD are in (b) and (d), respectively.

3(b)], i.e., $\mu_{GD} \cong \mu_1 + \mu_2$. Comparing Fig. 3(a) and 3(b), we find that the two plots are in quantitative agreement with each other.

Second, we calculate the following auxiliary function A, related to the molecular polarizability, which is defined as

$$A \equiv 2\sum_j \alpha_j^2 - 2\sum_{i<j} \alpha_i \alpha_j, \tag{14}$$

where α_1, α_2, and α_3 are the three diagonal elements when the *ab initio* calculated static (zero-frequency) molecular polarizability tensor, 3×3 matrix, is diagonalized—note that, even though the actual polarizability tensor required in the quantitative estimation of the light scattering cross section is dynamic polarizability at finite frequency of the incident radiation, the general trend can be well described by using the static polarizability tensor. The above orientationally averaged quantity, A, in Eq. (14) is related to the light scattering intensity I_T (obs. $\|$), where the incident radiation is directed in the Y direction and plane polarized along the X direction and the total intensity of the scattered radiation in the X direction is measured.[20] More specifically, the Rayleigh scattering intensity, I_T (obs. $\|$), is linearly proportional to the above auxiliary function, A, as

$$I_T(\text{obs.}\|) = \frac{16\pi^4\nu^4\rho I_0}{15c^4} A, \tag{15}$$

where ν is the frequency of the incident radiation, ρ the number density of the molecules, I_0 the incident flux of radiation, defined as $I_0 \equiv cE_0^2/8\pi$, and c the speed of light.

On the basis of the assumption that GD is a sum of NMA1 and NMA2, the molecular polarizability tensor of GD is given by a sum of two polarizabilities as $\alpha_{GD} \cong \alpha_{NMA1} + \alpha_{NMA2}$. In Figs. 3(c) and 3(d), the *ab initio* calculated $A_{GD}(\phi,\psi)$ and NMA-dimer-approximated $A_{GD}(\phi,\psi)$ functions are plotted and again the agreement between the two plots is quantitative. In summary, the dipole interaction model provides relatively poor results on the potential energy surface, but the spectroscopically relevant mo-

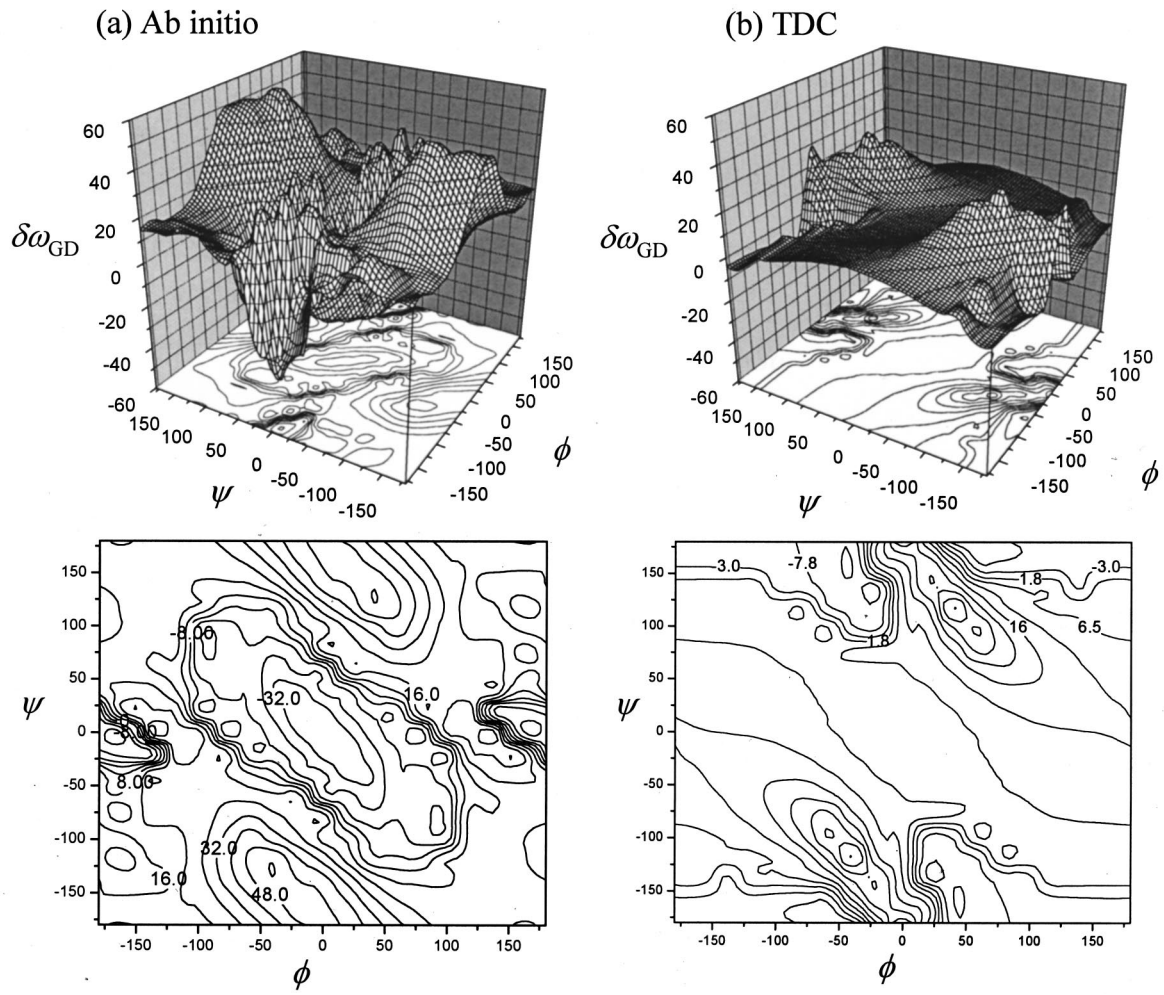

FIG. 4. $\delta\omega$ ($\delta\omega \equiv \omega_s - \omega_a$) in cm^{-1}. (a) *Ab initio* calculated $\delta\omega$. (b) The TDC-predicted $\delta\omega$.

lecular properties such as the permanent dipole moment and molecular polarizability of GD can be quantitatively calculated by using the NMA-dimer approximation.

B. Frequency splitting and center frequency

In Fig. 4(a), the *ab initio* calculated frequency splitting, $\delta\omega$, which is defined as $\delta\omega \equiv (\omega_s - \omega_a)$, is plotted in the (ϕ,ψ) space. Now, the TDC-predicted $\delta\omega$ by using the theoretical expression given in Eq. (10), with $\omega_1 = \omega_2$, is plotted in Fig. 4(b). Although the overall 3-D plots appear to be fairly different from each other (compare the two contour plots), the more relevant question is whether the TDC model prediction is quantitatively acceptable in the α-helical and β-sheet regions. In Table II, we compare the frequency splitting magnitude in these two conformational regions. Conclusively, the TDC model provides quantitatively acceptable results when the two peptides form an α-helical conformation, whereas the TDC model significantly underestimates the coupling force constant for β-sheet conformations. The latter feature, a failure of the TDC model for a β-sheet conformation of GD, cannot be easily explained, though Kubelka and Keiderling suggested that it is due to the relative orientation between the two peptides such that the two transition dipoles are canceled with each other.[21]

Next, the *ab initio* calculated center frequency, ω_{center}, defined as $\omega_{center} = (\omega_s + \omega_a)/2$, is plotted in Fig. 5(a). Depending on the molecular conformation, the center frequency, ω_{center}, varies from 1682 to 1770 cm^{-1}. The TDC-predicted ω_{center}, which is calculated by using Eq. (11), is plotted in Fig. 5(b). Here, the second derivative of the dipole moment of NMA with respect to the amide I vibrational coordinate, $\mu^{(2)}$ (in e/a_0), used to calculate C_{11} and C_{22} is found to be (0.3651, 0.0000, 0.9028). Although the magnitudes of C_{11} and C_{22} are quantitatively similar to the off-diagonal term, C_{12}, they are negligibly small in comparison to $\omega_1^2 (= \omega_2^2)$. Consequently, the center frequency, ω_{center}, within the dipole–dipole interaction model, is found to be almost constant around 1708 cm^{-1} [see Fig. 5(b)]. The result shows that the dipole–dipole interaction cannot account for the overall frequency shift of the amide I band when the structural conformation changes in the Ramachandran space. Therefore, the absolute frequencies of the symmetric and antisymmetric vibrational modes, not the frequency difference between the two, cannot be determined by using the dipole–dipole interaction model for a dipeptide, which is a fundamental assumption required in the TDC model. Currently, an alternative theoretical model taking into account the elec-

TABLE II. Frequency splitting ($\delta\omega \equiv \omega_s - \omega_a$) in α-helical and β-sheet regions calculated by the *ab initio* and the TDC model.

α helix	*Ab initio* (cm^{-1})			TDC (cm^{-1})		
$\psi\backslash\phi$	−80	−60	−40	−80	−60	−40
−40	16.84	9.66	2.25	14.59	12.08	8.89
−60	22.00	21.18	18.26	20.20	17.78	12.34
−80	27.43	33.09	26.81	23.37	27.36	17.92

β sheet	*Ab initio* (cm^{-1})				TDC (cm^{-1})			
$\psi\backslash\phi$	−180	−160	−140	−120	−180	−160	−140	−120
180	14.75	16.48	13.60	13.37	−4.02	−4.12	−4.42	−5.05
160	15.68	14.67	15.12	11.49	−3.87	−3.85	−4.05	−4.50
140	15.66	14.67	14.50	10.80	3.60	3.66	3.82	4.13
120	20.65	14.86	12.74	10.37	3.93	4.09	4.29	4.47
100	20.62	15.36	10.97	10.97	5.32	5.35	5.44	5.45
80	14.75	12.25	8.48	10.80	7.24	6.94	6.76	6.50
60	10.46	12.99	8.11	4.90	8.97	8.41	8.00	7.48

tronic change of a given peptide, when it is surrounded by other peptides or water, is being developed and will be presented elsewhere.[22]

C. IR and Raman intensities

As mentioned in Secs. III C and III D, the transition dipole and transition polarizability can be calculated by linear combinations of the local transition dipoles and local transition polarizabilities of the two unit peptides, respectively. For the *ab initio* calculated structures of GD, the absolute magnitudes of transition dipoles of the symmetric and antisymmetric modes, denoted as $|(\partial\mu_{GD}/\partial q_s)_0|$ and $|(\partial\mu_{GD}/\partial q_a)_0|$, are calculated and plotted in Figs. 6(a) and 6(b). In Figs. 6(c) and 6(d), the theoretically calculated $|(\partial\mu_{GD}/\partial q_s)_0|$ and $|(\partial\mu_{GD}/\partial q_a)_0|$ by using Eqs. (12a) and (12b) are plotted. Except for the region where the transition dipole coupling force constant is near zero, the two results are quantitatively in good agreement with each other. Therefore, the IR intensities of the symmetric and antisymmetric vibrational transitions can be well described by using the TDC theory presented in Sec. III.

We next consider the Raman intensities of the two amide I normal modes. To this end, an auxiliary function $B_m(\phi,\psi)$ (for $m=s$ and a) is defined as

$$B_m = 2\sum_j \left[\left(\frac{\partial\alpha}{\partial q_m}\right)_0\right]_j^2 - 2\sum_{i<j}\left[\left(\frac{\partial\alpha}{\partial q_m}\right)_0\right]_i\left[\left(\frac{\partial\alpha}{\partial q_m}\right)_0\right]_j. \tag{16}$$

The Raman scattering intensity, I_T (obs. $\|$), of a given vibrational mode is linearly proportional to the above function B. In Eq. (16), $[(\partial\alpha/\partial q)_0]_j$ for $j=1$, 2, and 3 are the three diagonal tensor elements, once the molecular transition polarizability tensor $(\partial\alpha/\partial q)_0$, which is a 3×3 matrix, is diagonalized. The *ab initio* calculated $B_s(\phi,\psi)$ and $B_a(\phi,\psi)$ are plotted in Figs. 7(a) and 7(b). The TDC-model-predicted $B_s(\phi,\psi)$ and $B_a(\phi,\psi)$ are depicted in Figs. 7(c) and 7(d). Again, the TDC model not only captures the general trends but also is quantitatively reliable in predicting the Raman intensities of the model dipeptide, GD.

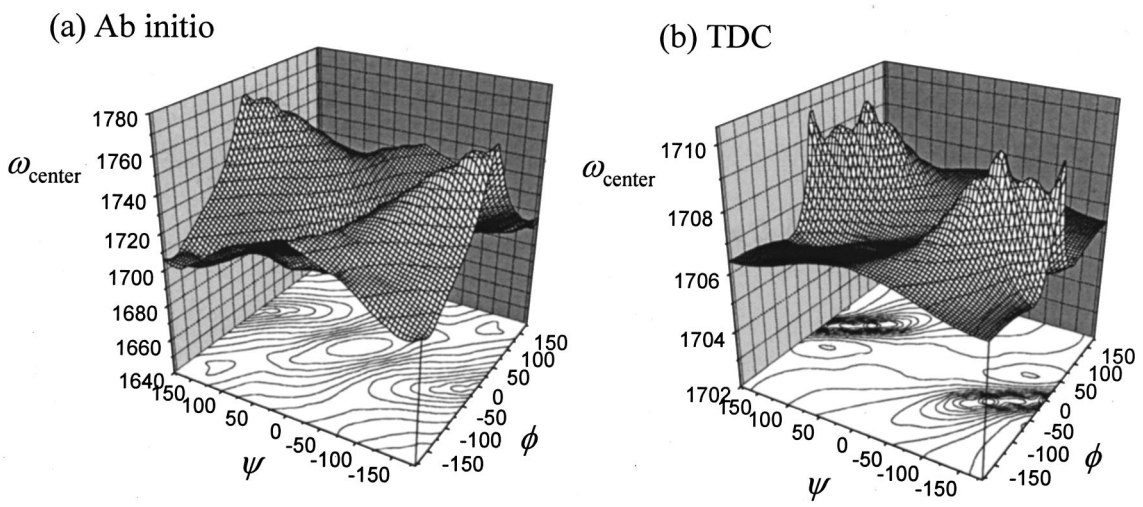

FIG. 5. The center frequency $\omega_{center}=(\omega_s+\omega_a)/2$ in cm^{-1}. (a) *Ab initio* calculation. (b) TDC. Note that the *z*-axis scale of (a) is much larger than that of (b).

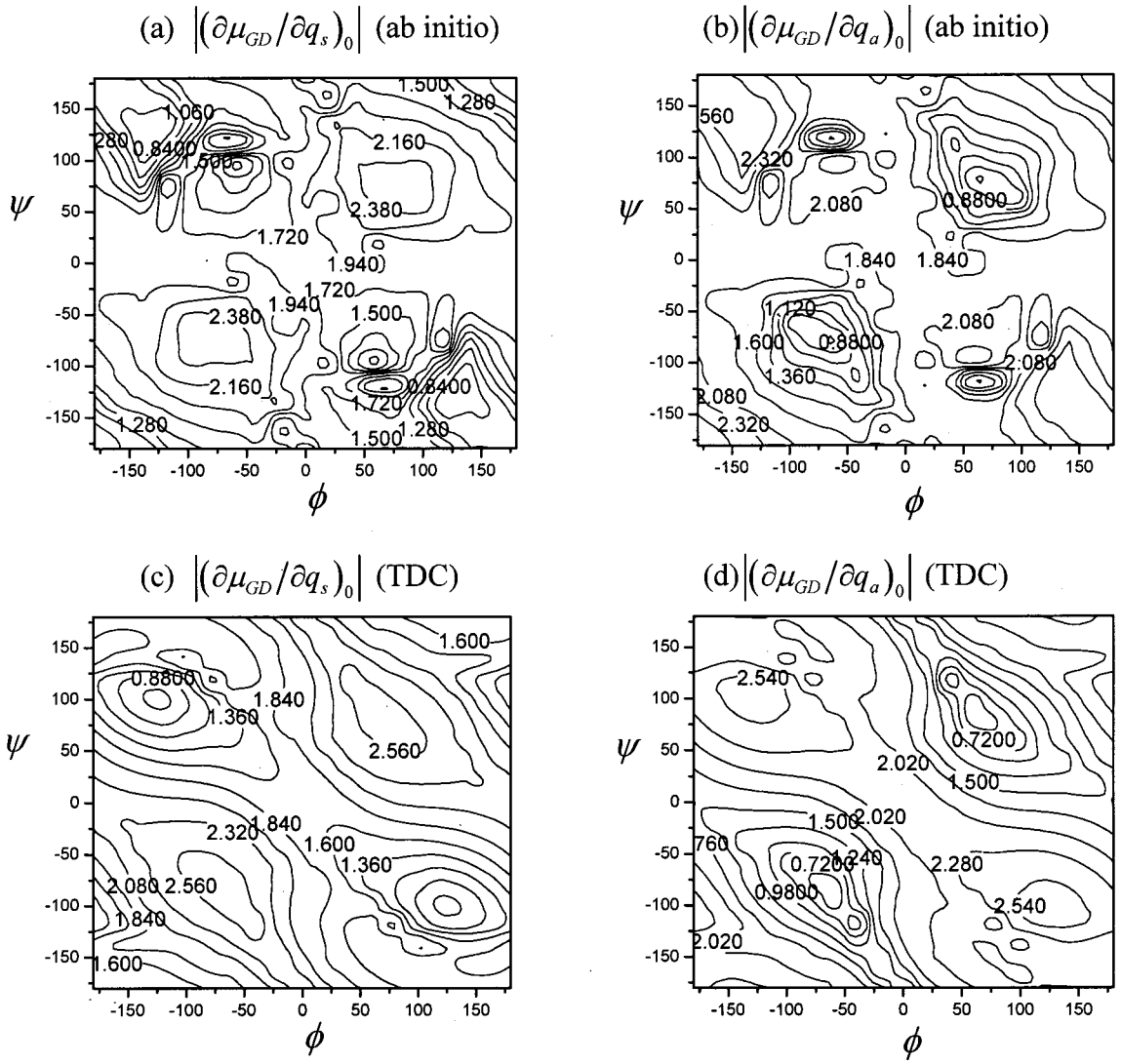

FIG. 6. Absolute magnitudes of transition dipoles (in e) of the symmetric and antisymmetric modes are shown in the (ϕ,ψ) space. (a) *Ab initio* data for the symmetric mode, (b) *ab initio* data for the antisymmetric mode, (c) TDC data for the symmetric mode, and (d) TDC data for the antisymmetric mode.

D. IR-Raman noncoincidence phenomenon

For polypeptides, the Raman noncoincidence phenomenon that the frequency of the amide I Raman band is different from that of the amide I IR band has been known very well.[23,24] This phenomenon can be easily understood by noting that the ratio of the IR intensity of the symmetric amide I vibration to that of the antisymmetric amide I vibration is different from the same ratio in the amide I Raman spectrum. In order to quantitatively discuss this noncoincidence phenomenon, we use the *ab initio* calculated results presented above. If the vibrational broadening is so large that the amide I IR and Raman bands appear to be a single peak, the center frequencies of the amide I IR and Raman bands can be calculated by using the following definitions:

$$\omega_{\mathrm{IR}}(\phi,\psi)\equiv\frac{|(\partial\mu_{\mathrm{GD}}/\partial q_s)_0|^2\omega_s+|(\partial\mu_{\mathrm{GD}}/\partial q_a)_0|^2\omega_a}{|(\partial\mu_{\mathrm{GD}}/\partial q_s)_0|^2+|(\partial\mu_{\mathrm{GD}}/\partial q_a)_0|^2}, \tag{17}$$

$$\omega_{\mathrm{Raman}}(\phi,\psi)\equiv\frac{B_s(\phi,\psi)\omega_s+B_a(\phi,\psi)\omega_a}{B_s(\phi,\psi)+B_a(\phi,\psi)}. \tag{18}$$

The *ab initio* calculated $\omega_{\mathrm{IR}}(\phi,\psi)$ and $\omega_{\mathrm{Raman}}(\phi,\psi)$ are depicted in Figs. 8(a) and 8(b), and the two plots are quantitatively similar to the center frequency, $\omega_{\mathrm{center}}(\phi,\psi)$, shown in Fig. 5(a). In order to see the noncoincidence phenomenon clearly, the frequency difference, defined as $\Delta\omega(\phi,\psi)\equiv\omega_{\mathrm{IR}}(\phi,\psi)-\omega_{\mathrm{Raman}}(\phi,\psi)$, is plotted in Fig. 8(c). We find that the IR-Raman noncoincidence frequency difference is about 5 cm^{-1} in both the α-helix and β-sheet regions.

V. INTERACTING PEPTIDES THROUGH SPACE: VALIDITY OF TDC THEORY

For a model dipeptide, a variety of molecular properties were calculated by using the *ab initio* calculation method and compared them with the TDC results. In this section, we further study the vibrational interaction between two formamides (FA) as a function of intermolecular distance between the two FAs. All geometrical parameters are fully optimized except (i) the intermolecular distance (r) and (ii) the relative orientation constraining the dimeric system to be a β-sheet-like structure [see Fig. 9(a)]. Similar to the GD molecule,

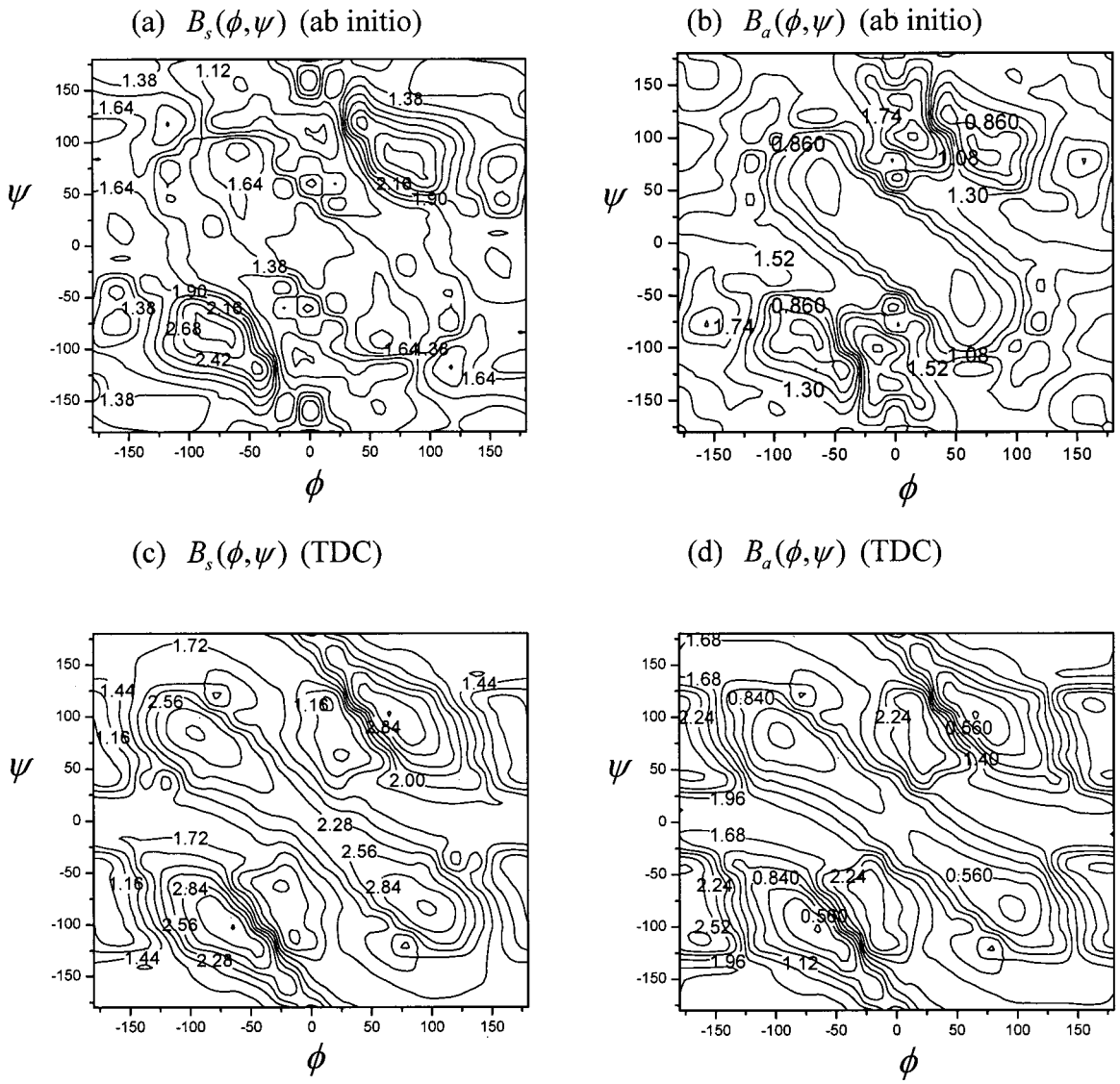

FIG. 7. B functions (in $e^4a_0^2/E_h^2$) of the symmetric and antisymmetric modes are shown in the (ϕ, ψ) space [see Eq. (16) and the main context for the definition of B function). (a) *Ab initio* calculated B_s of the symmetric mode, (b) *ab initio* calculated B_a of the antisymmetric mode, (c) TDC-calculated B_s of the symmetric mode, and (d) TDC-calculated B_a of the antisymmetric mode.

there are two amide I normal modes: symmetric and antisymmetric. The *ab initio* calculated frequency splitting magnitude as a function of r is plotted in Fig. 9(b), and it is approximately proportional to $1/r^3$. In order to use the TDC model, we carried out the *ab initio* calculation of a single FA molecule to obtain TDC parameters, such as the transition dipole *et al.* (see Table III). The magnitude of the transition dipole moment for FA is calculated to be 3.80 D Å^{-1} $\text{amu}^{-1/2}$ (17.7° from the CO axis and 0.868 Å from the carbonyl carbon atom). Although it is found that the TDC works very well as long as the distance between the two peptides is larger than 7 Å (which is close to the distance between the second nearest peptides), we find that the TDC underestimates the coupling force constant as the intermolecular distance decreases. In most of the previous reports utilizing the TDC model, the coupling force constant between two nearest-neighboring peptides was assumed to be successfully calculated by using *properly adjusted* TDC parameters, such as the transition dipole magnitude and orientation and origin of TD. However, recently Torii and Tasumi calculated coupling force constants for a tripeptide system and showed that one cannot use a *single set of TDC parameters* for quantitatively predicting the coupling force constant between two nearest-neighboring peptides as well as that between the second nearest peptides.[5] Here, it should be mentioned that their approach is critically different from ours. They first obtained a proper set of TDC parameters, such as the magnitude, orientation, and origin of TD of a single peptide, by fitting the calculated coupling force constant, C_{13}, between the second nearest-neighboring peptides (between the first and third peptides) with the TDC assumption. Then, thus obtained parameters were used to calculate the coupling force constant, C_{12}, between the nearest-neighboring peptides (between the first and second peptides) by the TDC theory and the comparison of TDC-predicted C_{12} with their *ab initio* calculated C_{12} showed an inadequacy of using a single set of TDC parameters to reproduce the *ab initio* calculation results. Also, they noted that the distance between two dipoles in a

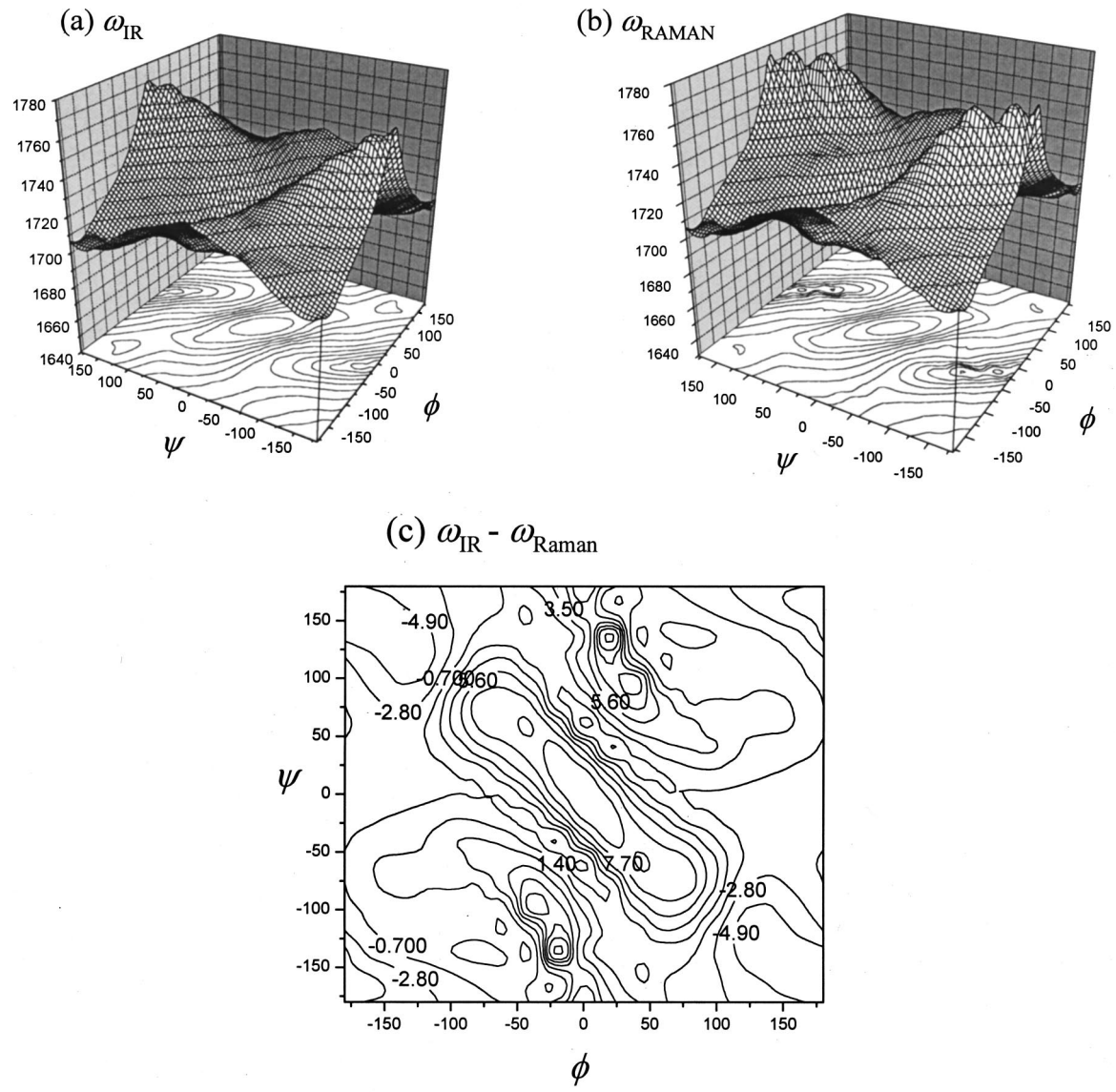

FIG. 8. Center frequencies (in cm^{-1}) of the amide I IR (a) and Raman bands (b) are shown. See Eqs. (17) and (18) for the definitions of ω_{IR} and ω_{Raman}. (c) The frequency difference between the two.

given dipeptide is so close that other factors contributing to the electrostatic interaction become important. The present calculation results, summarized in Fig. 9(b), strongly support their conclusions, though in our case the TDC parameters were obtained by solely using the *ab initio* calculation results of the unit peptide molecule, FA, instead of by using fitting procedure. Also, our observation that the TDC model underestimates the coupling force constant for a model

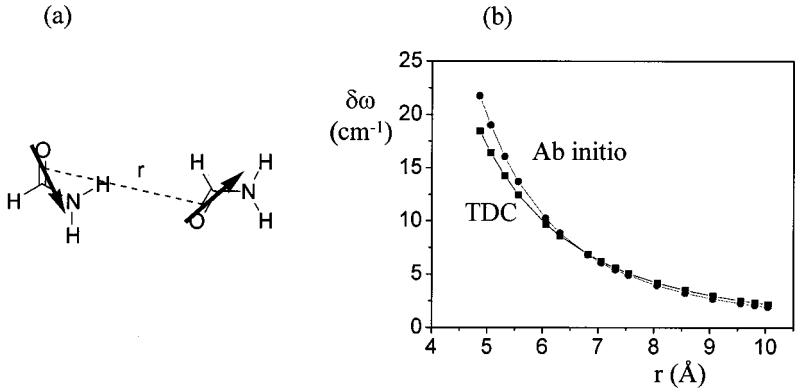

FIG. 9. (a) Two formamides separated by the intermolecular distance (in Å), *r*, between the centers of the transition dipoles. (b) $\delta\omega$ (in cm^{-1}) as a function of *r*.

TABLE III. Permanent dipole moment (in ea_0), polarizability tensor (in $e^4a_0^4/E_h^2$), transition dipole (in e), and transition polarizability tensor (in $e^4a_0^2/E_h^2$) of FA.

	μ	$(\partial\mu/\partial q)$
x	0.418	0.652
y	0.000	0.000
z	−1.604	−2.042
	α	$(\partial\alpha/\partial q)$
xx	22.117	−0.856
yx	0.000	0.000
yy	15.149	−0.135
zx	−2.453	−3.748
zy	0.000	0.000
zz	28.055	8.642

dipeptide in the β-sheet region (see Table II) is found to be consistent with the model calculation for a dimeric FA system presented in this section.

VI. SUMMARY

The transition dipole coupling model is based on the assumption that the interpeptide interaction is largely dictated by dipole–dipole interaction. Due to the simplicity of the TDC model, it has been extensively used to describe the amide I IR bands of a variety of polypeptides and proteins. Also, recently it has been widely used to numerically calculate two-dimensional IR pump–probe and photon–echo spectra of short polypeptides and globular proteins.[25–29] Woutersen and Hamm, for example, used the polarization sensitive 2-D IR pump–probe spectroscopy to extract information on the backbone structure of a trialanine in solution.[26] They were able to obtain the transition dipole coupling strength (β) and the relative angle (θ) between the transition dipole vectors of the two amide oscillators experimentally and compared them with the theoretically determined parameters in Fig. 4 in Ref. 26, which is comparable with Fig. 4(a) in the present paper. Although those numerical calculation results based on the TDC model and comparative investigations with experimental measurements were used to demonstrate the potential applicability of 2-D vibrational spectroscopies in the determination of a 3-D protein structure in the future, we believe that the numerical calculation results solely based on a TDC model should be carefully interpreted to make quantitative conclusions. In the present paper, we examined the validity of the dipole–dipole interaction model for a dipeptide, glycine dipeptide analog. In conclusion, we found that the model is successful in quantitatively calculating spectroscopic properties such as dipole moments, molecular polarizability, IR transition dipoles and intensity, and Raman transition polarizabilities of GD. On the other hand, the dipole–dipole interaction model is not quantitatively reliable in calculating potential energy surface and absolute frequencies of the amide I normal modes, though the TDC-predicted frequency splitting is quantitatively acceptable in the α-helix region. Currently, we are developing a mean field theoretical method to describe the frequency shift of the amide I vibration, i.e., diagonal force constant, for a dipeptide system and will present the results elsewhere.[22]

ACKNOWLEDGMENT

This work was supported by the Creative Research Initiatives Program of KISTEP (MOST, Korea).

[1] S. Krimm and J. Bandekar, Adv. Protein Chem. **38**, 181 (1986), and reference therein.
[2] S. Krimm and Y. Abe, Proc. Natl. Acad. Sci. U.S.A. **69**, 2788 (1972); W. H. Moore and S. Krimm, *ibid.* **72**, 4933 (1975).
[3] W. H. Moore and S. Krimm, Biopolymers **15**, 2465 (1976); A. M. Dwivedi and S. Krimm, Macromolecules **15**, 186 (1982); **16**, 340 (1983).
[4] H. Torii and M. Tasumi, J. Chem. Phys. **96**, 3379 (1992).
[5] H. Torii and M. Tasumi, J. Raman Spectrosc. **29**, 81 (1998).
[6] H. H. Mantsch, H. L. Casal, and R. N. Jones, in *Spectroscopy of Biological Systems, Advances in Spectroscopy*, Vol. 13, edited by R. J. H. Clark and R. E. Hester (Wiley, New York, 1986), p. 1.
[7] H. Torii and M. Tasumi, J. Chem. Phys. **97**, 92 (1992).
[8] H. Torii and M. Tasumi, J. Chem. Phys. **97**, 86 (1992).
[9] S. Krimm and J. W. C. Reisdorf, Faraday Discuss. **99**, 181 (1994).
[10] H. Torii, T. Tatsumi, and M. Tasumi, Mikrochim. Acta, Suppl. **14**, 531 (1997).
[11] H. Torii, T. Tatsumi, and M. Tasumi, J. Raman Spectrosc. **29**, 537 (1998).
[12] H. Torii and M. Tasumi, Int. J. Quantum Chem. **70**, 241 (1998).
[13] D. A. Dixon, K. D. Dobbs, and J. J. Valentini, J. Phys. Chem. **98**, 13435 (1994).
[14] N. G. Mirkin and S. Krimm, J. Am. Chem. Soc. **113**, 9742 (1991).
[15] A. Tu, in *Spectroscopy of Biological Systems*. edited by R. J. H. Clark and R. E. Hester (Wiley, Chichester, 1989), p. 47.
[16] M. J. Frisch, G. W. Trucks, H. B. Schlegel *et al.*, GAUSSIAN 98, Revision A.7 Gaussian, Inc., Pittsburgh, PA, 1998.
[17] L. Schafer, C. V. Alsenoy, and J. N. Scarsdale, J. Chem. Phys. **76**, 1439 (1982).
[18] V. J. Klimkowski, L. Schafer, F. A. Momany, and C. V. Alsenoy, J. Mol. Struct. **124**, 143 (1985).
[19] T. C. Cheam and S. Krimm, J. Mol. Struct. **193**, 1 (1989).
[20] D. A. McQuarries, *Statistical Mechanics* (Harper & Row, New York, 1976).
[21] J. Kubelka and T. A. Keiderling, J. Am. Chem. Soc. **123**, 6142 (2001).
[22] S. Ham and M. Cho (unpublished).
[23] J. Jonas and Y. T. Lee, J. Phys.: Condens. Matter **3**, 305 (1991).
[24] D. E. Logan, Chem. Phys. **131**, 199 (1989).
[25] A. Piryatinski, S. Tretiak, V. Chernyak, and S. Mukamel, J. Raman Spectrosc. **31**, 125 (2000).
[26] S. Woutersen and P. Hamm, J. Phys. Chem. B **104**, 11316 (2000).
[27] P. Hamm, M. Lim, and R. M. Hochstrasser, J. Phys. Chem. B **102**, 6123 (1998).
[28] C. Scheurer, A. Piryatinski, and S. Mukamel, J. Am. Chem. Soc. **123**, 3114 (2001).
[29] A. Piryatinski, V. Chernyak, and S. Mukamel, in *Ultrafast Infrared and Raman Spectroscopy*, edited by M. D. Fayer (Marcel Dekker, New York, 2001).